Discover Oncology

RESEARCH Open Access

Study on the in vitro and in vivo killing effects of PD-1 antibody-secreting c-Met-targeted CAR-T cells on esophageal cancer cell line ECA109

Shang Peng[1], Yanqiu Li[1], Yanjun Zhang[2], Jingting Min[1], Ran An[3], Nana Du[1], Haipeng Li[4], Xiangcheng Zhen[5], Fei Chu[1] and Zhenghong Li[2*]

*Correspondence:
Zhenghong Li
lzhbbmc@126.com
[1]Department of Basic Medical, Bengbu Medical University, Bengbu, AH, China
[2]Department of Life Sciences, Bengbu Medical University, Bengbu, AH, China
[3]Department of Public Foundations, Bengbu Medical University, Bengbu, AH, China
[4]Department of Mental Health Medical, Bengbu Medical University, Bengbu, AH, China
[5]Department of Clinical Medical, Bengbu Medical University, Bengbu, AH, China

Abstract

Background This study was designed to investigate the in vitro and in vivo killing effects of PD-1 antibody-secreting c-Met-targeted CAR-T cells on esophageal cancer cell line ECA109.

Methods We employed the TCGA and GTEx databases to analyze the expression levels of c-Met and PD-L1 in esophageal cancer tissues. Immunohistochemistry was employed to detect the expression of c-Met and PD-L1 in clinical esophageal cancer tissues and adjacent normal tissues. Flow cytometry was employed to verify the expression of c-Met and PD-L1 in ECA109 cells. T cells from healthy volunteers were extracted and activated, and c-Met/PD-1 CAR-T cells were prepared utilizing lentivirus. Flow cytometry was employed to detect the positive rate, subtype, antibody secretion, and anti-apoptotic effects of c-Met/PD-1 CAR-T cells. The experimental group consisted of c-Met/PD-1 CAR-T cells, with c-Met CAR-T and CD19 CAR-T as control groups, and Active T cells as the blank control group. The proliferation, cytokine secretion, and killing ability of CAR-T cells co-cultured with ECA109 cells were assessed utilizing cell viability assays (CCK-8), enzyme-linked immunosorbent assays (ELISA), and lactate dehydrogenase release assays (LDH). In vivo experiments were conducted by subcutaneously injecting ECA109 cells into nude mice to establish tumor-bearing models. CAR-T cells were administered via in situ injection, and changes in body weight and tumor volume were measured. Hematoxylin and eosin (HE) staining was performed on heart, liver, spleen, lung, and kidney tissues from sacrificed mice.

Results c-Met and PD-L1 were highly expressed in esophageal cancer tissues but were low or not expressed in adjacent normal tissues. ECA109 cells expressed c-Met and PD-L1 on their surface. Successfully prepared c-Met/PD-1 CAR-T cells secreted PD-1 antibodies that blocked PD-1 on the surface of CAR-T cells. Under stimulation by c-Met antigens, c-Met/PD-1 CAR-T cells exhibited stronger proliferation, cytokine release, and killing ability. In vivo experiments demonstrated significant tumor inhibition in nude mice treated with c-Met/PD-1 CAR-T cells without evident off-target effects.

Conclusion The c-Met/PD-1 CAR-T cells were successfully constructed and demonstrated significant in vitro and in vivo killing effects on ECA109 esophageal cancer cells.

Keywords Esophageal cancer, Chimeric antigen receptor T cells, c-Met, PD-1 antibody

1 Introduction

Esophageal carcinoma (ESCA) is one of the most common malignancies of the digestive tract. Currently, surgical resection is considered the first choice for patients. However, early diagnosis of esophageal cancer is challenging due to the rich lymphatic drainage in the submucosa, leading to early lymph node metastasis. Consequently, most patients are diagnosed at advanced or metastatic stages [1]. For advanced esophageal cancer, the median survival time is 12 to 18 months, with a 5-year survival rate of 15–39% [2, 3]. Recurrence, either local or systemic, is common, affecting 35–50% of patients who undergo surgery alone [4]. Radiotherapy and chemotherapy offer poor efficacy for ESCA patients, necessitating new strategies to improve treatment outcomes and quality of life.

CAR-T cell therapy has achieved encouraging clinical results in treating hematologic malignancies [5, 6]. However, the clinical efficacy of CAR-T cells in solid tumors has been disappointing, mainly due to tumor-specific antigens and immune escape mechanisms [7]. CAR-T cells can specifically recognize tumor surface antigens, ensuring they attack only tumor cells without harming normal tissues. However, tumors often evade immune recognition by downregulating or losing surface antigens. For instance, CD19 CAR-T cell therapy for B-cell lymphoma has shown that up to 60% of relapses are characterized by CD19 antigen loss [8]. While tumor-specific antigens (TSAs) are rare in solid tumors [9], tumor-associated antigens (TAAs) are more common, posing a potential risk of targeting non-tumor tissues [10].

The cellular-mesenchymal epithelial transition factor (c-Met) is widely expressed in various cancers, including lung, colon, and ovarian cancers [11]. It promotes tumor cell proliferation, migration, and invasion, leading to tumor growth and metastasis. c-Met has become a clinical detection marker for tumors, with several c-Met-targeted drugs, such as Tepotinib, Capmatinib, Rybrevant, and Rilotumumab, achieving significant results [12]. Studies have reported that c-Met-targeted drugs like Rilotumumab, combined with chemotherapy, benefit esophageal cancer patients [13], especially those with high c-Met expression [14]. c-Met is highly expressed in esophageal cancer and is considered an independent prognostic factor and potential therapeutic target. However, while c-Met is a promising target, there is currently no literature validating the killing effect of c-Met CAR-T cells on esophageal cancer cells. Despite this, c-Met's broad and specific expression in tumors continues to make it an increasingly attractive target for CAR-T therapy. By enabling T cells to effectively target and kill tumor cells while minimizing off-target effects, c-Met CAR-T therapy holds significant promise. In preclinical studies, c-Met CAR-T has demonstrated tumor-suppressive effects in various solid tumors, including non-small cell lung cancer (NSCLC) [15], hepatocellular carcinoma (HCC) [16], and gastric cancer (GC) [17], further highlighting its potential to improve clinical outcomes, particularly in cancers that express high levels of c-Met.

The immune checkpoints in the tumor microenvironment lead to immune cell exhaustion and immune escape. This issue can potentially be addressed utilizing immune checkpoint inhibitors. Immune checkpoints are inhibitory molecules expressed on

immune cells, negatively regulating immune activation to prevent autoimmunity and hypersensitivity. T cells are the main force of tumor immunity [18], with cancer cells' programmed death ligand 1 (PD-L1) recognizing and activating the programmed death 1 (PD-1) receptor on tumor-infiltrating T cells, cautilizing T cell exhaustion and apoptosis, leading to tumor immune escape. Immune checkpoint inhibitors effectively unleash immune factors, maximizing immune capacity and preventing immune escape while killing tumors. PD-1/PD-L1 pathway inhibitors are widely employed in esophageal cancer, disrupting this pathway and allowing Active T cells to attack cancer cells [19]. Several global and domestic drugs have been approved for esophageal cancer treatment. The 2023 NCCN and CSCO guidelines recommend multiple PD-1/PD-L1 immune checkpoint inhibitors for first-line or second-line esophageal cancer treatment [20]. In recent reports, Akeso Biopharma has developed Ivonescimab, a bispecific monoclonal antibody that combines PD-1 inhibition with vascular endothelial growth factor (VEGF)-A targeting [21]. Thanks to the addition of the PD-1 antibody, Ivonescimab has shown significant improvements in progression-free survival (PFS) in patients with non-small cell lung cancer (NSCLC), cholangiocarcinoma, and other solid tumors. In the phase III HARMONI-A trial, the combination of Ivonescimab with chemotherapy significantly prolonged PFS by 2.3 months compared to the placebo plus chemotherapy group. This highlights the growing potential of combining PD-1 inhibition with other therapeutic strategies to improve clinical outcomes in solid tumors.

Thus, this study was designed to construct PD-1 antibody-secreting c-Met CAR-T cells (c-Met/PD-1 CAR-T), which secrete PD-1 blocking antibodies extracellularly, binding to their PD-1 sites and blocking the PD-1/PD-L1 pathway. We successfully constructed c-Met/PD-1 CAR-T cells, which demonstrated superior anti-tumor effects on esophageal cancer cell line ECA109 in vitro and in vivo compared to c-Met CAR-T cells.

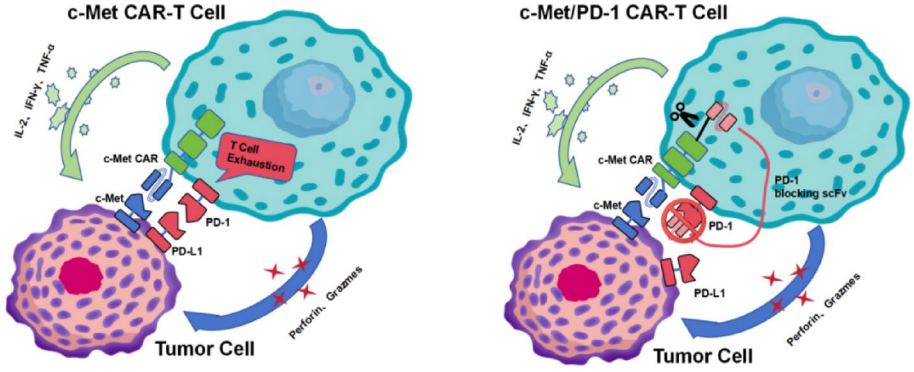

Comparison of c-Met CAR-T and c-Met/PD-1 CAR-T cell mechanisms. Left: c-Met CAR-T cells induce T cell exhaustion via PD-1/PD-L1 signaling. Right: c-Met/PD-1 CAR-T cells secrete PD-1 blocking scFv, preventing exhaustion and enhancing anti-tumor efficacy through cytokine secretion

2 Materials and methods

2.1 Gene expression analysis

Human tumor gene atlas (TCGA) and genotype-tissue expression (GTEx) RNA data in TPM format were downloaded from UCSC XENA and analyzed. Esophageal cancer data from TCGA and corresponding normal tissue data from GTEx were extracted. MET gene expression data from ESCA and normal tissues were sourced from the TCGA and

GTEx databases and processed using the UCSC Xena tool. Gene expressions were standardized to transcripts per million (TPM).

We analyzed the expression of MET, PDCD1, CD274, and six other reported CAR-T targets (EGFR, EPHA2, MUC1, CD276, ERBB2) in cancerous and normal tissues, utilizing normal tissue data from the GTEx database, which includes samples from healthy individuals without cancer. Using the "limma" and "ggplot2" R packages, we compared and visualized the gene expression between cancerous and normal tissues. By comparing the TPM of each target gene in tumor and adjacent normal tissues, we calculated the Tumor Ratio to assess the specificity of the targets.

2.2 Tissue specimens and immunohistochemistry

This study was approved by the Ethics Committee of Bengbu Medical University (Approval No. Lunke [2022] No. 115). With the approval of the Ethics Committee, tumor and adjacent tissue samples were collected from 150 newly diagnosed, untreated esophageal cancer patients who underwent surgical resection between 01/01/2017 and 01/01/2023.All tissue samples were anonymized before use in this study, and no identifiable personal information was accessed during or after the research. The Ethics Committee waived the need for additional informed consent for the use of these archived samples in retrospective research. All tissue samples were anonymized prior to use in this study. All samples were fixed in 4% neutral formalin, embedded in paraffin, and sectioned to a thickness of 4 μm. Following deparaffinization, rehydration, cell permeabilization, antigen retrieval, and serum blocking, primary antibodies against c-Met (proteintech# 25869-1-AP) and PD-L1 (proteintech# 17952-1-AP) were diluted 1:2000 and applied to the slides. Incubation was carried out at 4 °C for 16 h. Afterward, the slides were incubated with goat anti-rabbit secondary antibody for 15 min. Staining was visualized using DAB, and the slides were subjected to dehydration through a graded ethanol series, followed by xylene clearing, and finally mounted with neutral resin. The results were evaluated under a microscope. Two qualified pathologists, blinded to the clinical data, independently assessed the results. Both c-Met and PD-L1 are transmembrane proteins, and their positivity was determined by the presence of brownish-yellow granules in the cytoplasm and cell membrane. The evaluation criteria were based on the percentage of positive cells and staining intensity. The positivity rate was scored as follows: 0 points (0%), 1 point (0–10%), 2 points (10–50%), and 3 points (> 50%). Staining intensity was graded as: 0 points (no staining), 1 point (weak staining), 2 points (moderate staining), and 3 points (strong staining). The final score was calculated by multiplying the positivity rate score by the staining intensity score. A total score of 0–1 was considered negative (-), 2 was considered equivocal (±), 3–5 was considered positive (+), 6–8 was considered strongly positive (++), and a score greater than 8 was considered highly positive (+++).

2.3 Cell lines

The human esophageal cancer cell line ECA109 was purchased from Hefei Wanwu Biotechnology and preserved in our laboratory. ECA109 cells expressing firefly luciferase (ECA109-luc) were established via lentiviral transduction. Cells were cultured in RPMI-1640 medium (Gibco#11875119) supplemented with 10% fetal bovine

serum (Gibco#A5670801), 100 mg/ml penicillin, and 100 mg/ml streptomycin (Gibco#15140148) at 37 °C in a 5% CO2 incubator.

2.4 Construction of the c-Met/PD-1 CAR

The c-Met scFv gene sequence and PD-1 antibody secretion gene sequence were obtained from patent databases (patent numbers CN 104159909 A, WO 2016210129 A1). The GV401 lentiviral vector plasmid was selected, with the PD-1 antibody secretion sequence linked to CD3ζ via FP2A. The plasmid synthesis process was completed by GeneChem (Shanghai, China).

2.5 Preparation of c-Met/PD-1 CAR-T

Peripheral blood mononuclear cells (PBMCs) were isolated from healthy volunteers and activated with mouse anti-CD3/CD28 antibodies (Gibco#16-0037-81, 16-0289-81). Active T cells were infected with lentivirus at a multiplicity of infection (MOI) of 5 in the presence of Retronectin. c-Met CAR-T, CD19 CAR-T, and Active T cells were also prepared and cultured in recombinant humanIL-2 (Abcam#ab119439), IL-7 (Abcam#ab259382), and IL-15 (Abcam#ab259403).

2.6 Detection of cell surface biomarkers

Flow cytometry was performed to detect target expression on esophageal cancer ECA109 cells using c-Met-FITC (1:200, Invitrogen#11-8858-42) and PD-L1-PE (1:200, Invitrogen#12-5983-42). Active T cell surface molecular markers were analyzed using PD-1-PE (1:200, Invitrogen#MA5-28583) and His-PE (1:200, Genscript#A02247).

2.7 Detection of c-Met / PD-1 CAR-T cells

Flow cytometry was used to detect the positive rate of CAR-T. Since the GV401 vector carried the eGFP marker gene, the flow cytometry FITC channel could be used to measure the CAR-T infection efficiency. The second-generation c-Met CAR-T and fourth-generation c-Met / PD-1 CAR-T were collected 2×10^5 each, and the negative control CD19 CAR-T and blank control activated T cells were collected 2×10^5 each. After PBS washing three times, flow cytometry was used to detect. Western blot was used to detect the secretion of PD-1 antibody in the fourth generation of c-Met / PD-1 CAR-T. Since the secreted PD-1 antibody carries the HIS tag and forms a fusion protein with it, the secretion of PD-1 antibody can be verified by detecting the HIS tag in the cell supernatant. T cell supernatant cultured with commercial recombinant HIS-tag PD-1 ScFv antibody was added as positive control. The cell supernatant after 24 h of culture was centrifuged to remove the precipitate, and the protein was separated by PAGE gel electrophoresis. The target molecular weight protein was transferred to the PVDF membrane, blocked with 5% skimmed milk powder for 1 h, and incubated with mouse anti-human HIS primary antibody (Proteintech#66005-1-Ig,1:1000) overnight at 4 °C. After washing, rabbit anti-mouse HRP coupled secondary antibody was incubated for 2 h, and the color solution was added dropwise and visualized by ECL exposure.

The distribution of CAR-T cell subsets was detected by flow cytometry. The second-generation c-Met CAR-T and the fourth-generation c-Met / PD-1 CAR-T were collected, 2×10^5 each. The negative control CD19 CAR-T and the blank control activated T cells were collected, 2×10^5 each. After washing with PBS, 5 μl of APC-CD3 (1:200,

Invitrogen#17-0037-42), PE-CD4 (1:200, Invitrogen#12-0049-42) and Pre-PC5.5-CD8 (1:200, Invitrogen#45-0088-42) antibodies were added to each group. At the same time, the activated T cells were used to set up three kinds of antibody single positive tubes to adjust the voltage, and incubated at 4 °C in dark for 30 min. Flow cytometry was used for detection. Analyze all data using Flowjo V12.

2.8 Functional verification of PD-1 ScFv

c-Met/PD-1 CAR-T cells and Active T cells cultured for six days were collected, resuspended in 1 ml of complete medium (without cytokines), and adjusted to a concentration of 1×10^6 cells/ml. A total of 1 ml of the cell suspension was seeded into a 6-well plate. At this stage, c-Met/PD-1 CAR-T cells secreted PD-1 scFv, whereas Active T cells did not. After 24 h, the supernatant was collected by centrifugation.

Subsequently, Active T cells were resuspended separately in supernatants containing or lacking PD-1 scFv and then co-cultured with adherent ECA109 cells in a 24-well plate at an effector-to-target (E: T) ratio of 1:1 for 24 h. Following incubation, all Active T cells were collected from the system and stained using an apoptosis detection kit(Beyotime#C1062S) to assess T cell apoptosis and evaluate the protective effect of PD-1 scFv.

2.9 Detection of CAR-T cell proliferation in vitro

1×10^4 tumor cells ECA109 were co-cultured with 1×10^4 effector cells for 24 h, 48 h and 72 h, and the final volume was 200 μl. After the culture, the suspended T cells and non-adherent cancer cell debris were washed away, and the medium was supplemented to a final volume of 200 μl. At the same time, the same number of co-culture unwashed holes were set up. All holes were added with 0.1 times the volume of CCK-8 reagent (Beyotime#C0037), and incubated at 37 °C for 2 h in the dark. The OD value of each measuring hole was detected by microplate reader, and the initial (0 h) OD value of each effector cell was detected. The number of cells at each time point in each group = 1×10^4×(unwashed hole OD value-washed hole OD value) / 0 h effector cell OD value.

2.10 Cytokine release assays

The amount of cytokines IL-2, TNF-α and IFN-γ released by effector cells in the presence of target cells was detected by enzyme-linked immunosorbent assay(Beyotime#m1058063V, m1064303V, m1057856V). Each group was added with 1×10^6 effector cells and 1×10^6 tumor cells in a 96-well plate, respectively, and co-cultured for 24 h. The culture system was 5% fetal bovine serum + 95% 1640 medium, and the final volume was 200 μl. The supernatant of the cells was centrifuged and diluted 5 times, and the concentrations of IL-2, TNF-α and IFN-γ were detected according to the ELISA kit instructions.

2.11 Cytotoxicity assays

The cytotoxicity of CAR-T cells was detected by lactate dehydrogenase release kit(Beyotime#C0018S). The effector cells and tumor cells in each group were incubated in 2% horse serum 1640 medium for 6 h, and the final volume was 200 μl. The number of tumors was constant at 1×10^4, and effector cells were added to each group according to

the gradient effect-target ratio (1 : 1, 5 : 1, 10 : 1 and 20 : 1) (experimental group 1 : c-Met CAR-T; experimental group 2 : PD-1 / c-Met CAR-T; control group 1 : CD19 CAR-T; control group 2 : activated T cell), set up target cells, effector cells natural release holes, target cells maximum release holes and blank holes respectively, and 20 μl LDH release reagent was added to the maximum release hole of target cells 1 h before the end of co-culture. The detection solution was configured according to the instructions. The 120 μl cell supernatant and 60 μl detection solution were mixed in a new 96-well plate, incubated at room temperature for 30 min, and the OD value of each well was detected by a microplate reader.The formula is as follows : killing efficiency % = (OD value of co-culture hole-OD value of natural release hole of effector cells-OD value of natural release hole of target cells + OD value of blank hole) / (OD value of maximum release hole of target cells-OD value of natural release hole of effector cells).

2.12 In vivo experiments

Four-week-old Balb/c nude mice, purchased from JicuiKang Biological Technology Co., Ltd. (Nanjing, China), were housed in a specific pathogen-free (SPF) barrier system and monitored daily. The timeline is shown in Fig. 7C. Mice were subcutaneously injected with 1×10^7 ECA109-Luc cells to establish tumor models and were divided into four groups: c-Met/PD-1 CAR-T, c-Met CAR-T, Active T cells, and PBS. On days 14 and 21, 1×10^7 CAR-T cells were administered to each group.Since the actual effector-to-target (E:T) ratio within the tumor is dynamic and difficult to control, the E:T ratio of 1:1 used in the in vivo experiments was based on the initial injection of tumor cells and CAR-T cells. Tumor volume and body weight were measured every three days. On day 28, mice were sacrificed using an overdose of sodium pentobarbital (200 mg/kg) to ensure a humane death, and death was confirmed. HE staining was performed on heart, liver, spleen, lung, and kidney tissues. Throughout the study, no mice exhibited poor health or mortality. All animal experiments were conducted in accordance with the ARRIVE guidelines.

2.13 Statistical evaluations

The measurement data were expressed as mean ± standard deviation ($x \pm s$), and the count data were expressed as percentage (%). SPSS 23.0 software was used for statistical analysis. For comparisons among multiple groups, one-way analysis of variance (ANOVA) was performed. When significant differences were identified by ANOVA, pairwise comparisons were conducted using a t-test. For experiments involving time-series data, a two-way analysis of variance (ANOVA) was applied to assess the effects of time and treatment, followed by Tukey's HSD (Honestly Significant Difference) test for post-hoc analysis. The significance level was set at $p < 0.05$.

3 Results

3.1 Gene expression analysis

Bioinformatics Validation of c-Met, PD-1, and PD-L1 Gene Expression in ESCA Analysis of TCGA data (Fig. 1A), paired TCGA samples (Fig. 1B), and combined TCGA-GTEx data (Fig. 1C) revealed that the expression levels of MET, PDCD1, and CD274 were significantly increased in tumor tissues compared to adjacent normal tissues ($p < 0.05$).

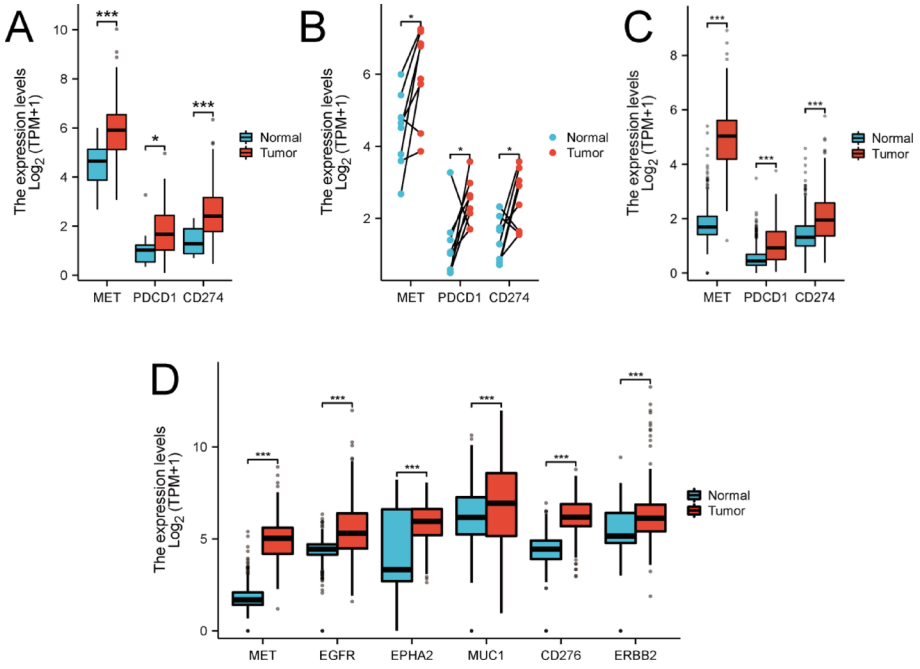

Fig. 1 Expression of MET, PDCD1, and CD274 in Esophageal Cancer. **A** Box plot of differential expression of MET, PDCD1, and CD274 in esophageal cancer (TCGA database) analyzed by one-way ANOVA,*p < 0.05, ***p < 0.001; **B** Line plot of paired analysis of differential expression of MET, PDCD1, and CD274 in esophageal cancer (TCGA database)analyzed by paired t-test, *p < 0.05; **C** Box plot of differential expression of MET, PDCD1, and CD274 in esophageal cancer (TCGA combined with GTEx database)analyzed by one-way ANOVA, ***p < 0.001; **D** Box plot of differential expression of MET and known CAR-T targets in esophageal cancer (TCGA combined with GTEx database)analyzed by one-way ANOVA, ***p < 0.001

Table 1 Expression levels of each target in tumor and adjacent normal tissues

Gene name	Average Expression in tumor Tissue (Unit: Log2(TPM + 1))	Average Expression in Adjacent Tissue (Unit: Log2(TPM + 1))	Tumor ratio
MET	4.97	1.79	2.77
EGFR	5.48	4.38	1.25
EPHA2	5.87	4.42	1.33
MUC1	6.92	6.20	1.11
CD276	6.16	4.38	1.41
ERBB2	6.37	5.47	1.17

Table 2 Expression of c-Met in esophageal cancer and adjacent normal esophageal tissues

Tissue type	c-Met Pathology Score					
	-	±	+	++	+++	Total
Esophageal cancer	4	4	8	15	9	40
Adjacent tissue	13	4	3	0	0	20

Moreover, among known ESCA CAR-T targets (EGFR, EHPA2, MUC1, CD276, ERBB2), MET exhibited the highest tumor-to-normal expression ratio (Fig. 1D; Table 1).

3.2 Protein expression of c-Met and PD-L1 in esophageal cancer

Protein Expression of c-Met and PD-L1 in ESCA Immunohistochemical results demonstrated that c-Met was positively expressed in 35% of adjacent normal esophageal tissues and 90% of esophageal cancer tissues (Table 2; Fig. 2A–F). PD-L1 was positively expressed in 7% of adjacent normal tissues and 86% of esophageal cancer tissues

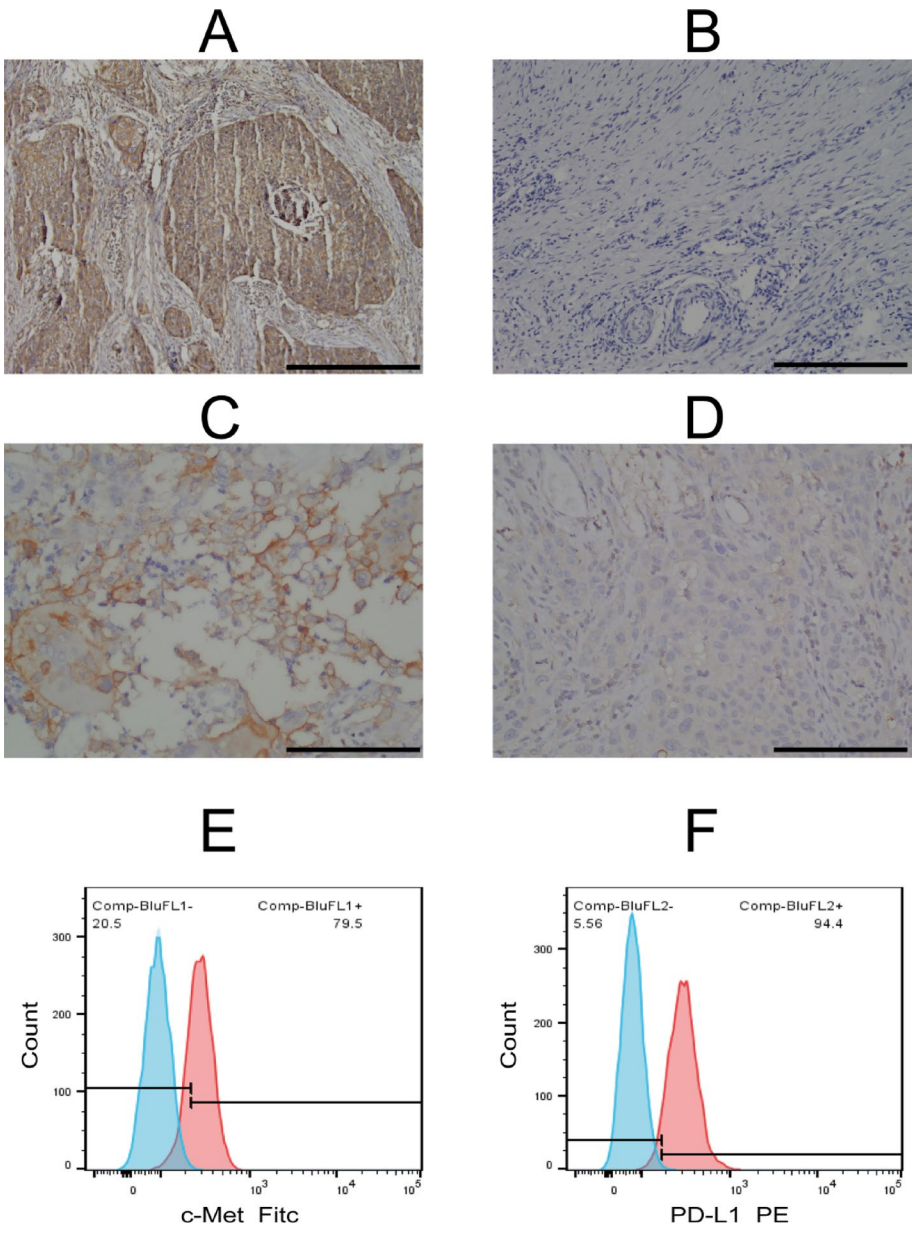

Fig. 2 Validation of c-Met and PD-L1 Protein Expression in Esophageal Cancer. **A** Immunohistochemical staining of c-Met in clinical esophageal cancer tumor samples (×400); **B** Immunohistochemical staining of c-Met in adjacent normal esophageal tissue samples (×400); **C** Immunohistochemical staining of PD-L1 in clinical esophageal cancer tumor samples (×400); **D** Immunohistochemical staining of PD-L1 in adjacent normal esophageal tissue samples (×400); **E** Flow cytometry analysis of c-Met expression on the surface of ECA109 cells. **F** Flow cytometry analysis of PD-L1 expression on the surface of ECA109 cells

(Table 3; Fig. 2G–L). Flow cytometry confirmed high expression of c-Met and PD-L1 on ECA109 cells (Fig. 2M).

3.3 Designing and identification of the c-Met/PD-1 CAR lentivirus expression plasmid

The c-Met/PD-1 CAR gene fragment (Fig. 3A) consisted of CD8α signal peptide, c-Met scFv, CD8α hinge region, CD8α transmembrane region, 4-1BB, CD3ζ, FP2A, CD8α signal peptide, PD-1 antibody, HIS tag, and EGFP. BamHI digestion and agarose gel

Table 3 Expression of PD-L1 in esophageal cancer and adjacent normal esophageal tissues

Tissue type	PD-L1 Pathology Score					
	-	±	+	++	+++	Total
Esophageal cancer	16	18	58	6	20	118
Adjacent tissue	28	2	0	0	0	30

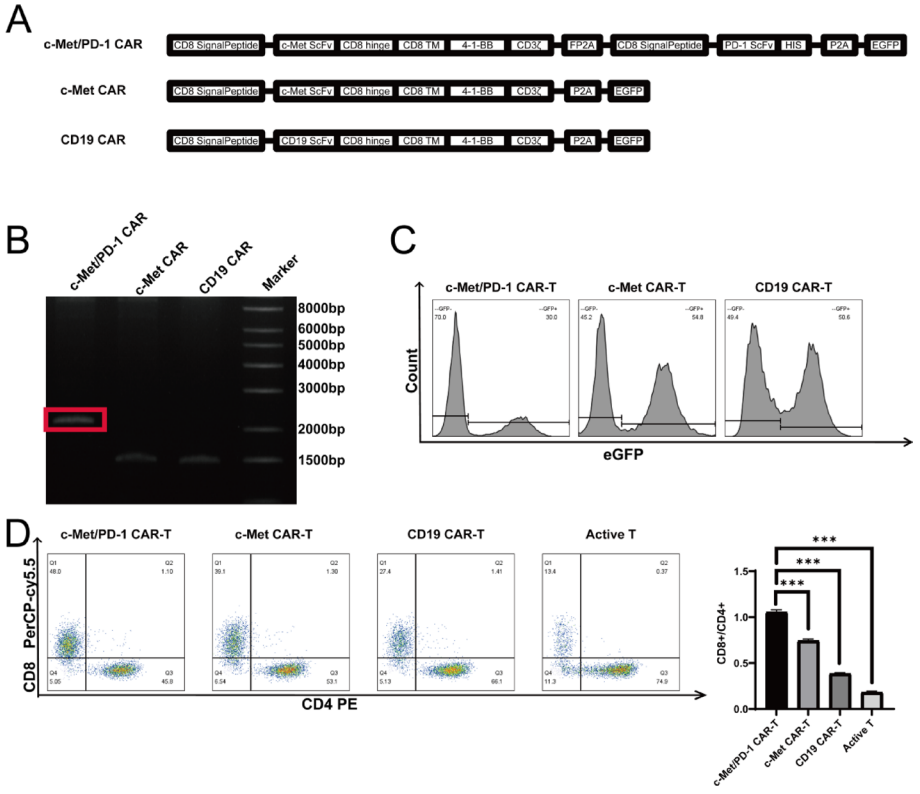

Fig. 3 CAR-T Design, Preparation, and Detection. **A** Schematic diagram of the core structures of c-Met/PD-1 CAR, c-Met CAR, and CD19 CAR; **B** Electrophoresis gel image of BamHI digestion of c-Met/PD-1 CAR(2436 bp), c-Met CAR(1498 bp), and CD19 CAR(1453 bp) plasmids; **C** Histogram showing the transfection efficiency of c-Met/PD-1 CAR-T, c-Met CAR-T, and CD19 CAR-T; D: Dot plot of CAR-T cell subset distribution, analyzed by one-way ANOVA (***$p < 0.001$, $n = 3$)

electrophoresis confirmed the expected size of the CAR scFv fusion fragment (2480 bp) (Fig. 3B).

3.4 Production of c-Met/PD-1 CAR-T cells

After 48 h of lentiviral transduction, EGFP was successfully expressed in the T cells and detected via the FITC channel (Fig. 3C). The positive rate of c-Met/PD-1 CAR-T cells reached 30%, while the positive rates of the control groups, c-Met CAR-T and CD19 CAR-T, were 54% and 50%, respectively. The proportions of CD8 + and CD4 + cells changed under the influence of the lentivirus (Fig. 3D). Flow cytometry analysis, gated on CD3 + cells, demonstrated that the CD8+/CD4 + ratio for c-Met/PD-1 CAR-T cells was 1.05 ± 0.03, compared to 0.74 ± 0.02 for c-Met CAR-T, 0.38 ± 0.01 for CD19 CAR-T, and 0.18 ± 0.01 for Active T cells. The CD8+/CD4 + ratio in c-Met/PD-1 CAR-T cells was the highest among the groups, with the difference being statistically significant ($P < 0.001$).

3.5 Detection of PD-1 antibody

Western blot demonstrated a 25 kDa HIS protein in the supernatant of c-Met/PD-1 CAR-T cells, consistent with the expected molecular weight (Fig. 4A). Flow cytometry confirmed HIS tag expression only in the supernatant of c-Met/PD-1 CAR-T cells. In addition, HIS tags could be detected on Active T cells after co-incubation with the supernatant of c-Met/PD-1 CAR T cells (Fig. 4B). The mean fluorescence intensity of PD-1 on c-Met/PD-1 CAR-T cells was significantly decreased than that on c-Met CAR-T, CD19 CAR-T, and Active T cells ($P < 0.05$) (Fig. 4C).

3.6 Detection of T cell apoptosis

After co-culturing Active T cells with cancer cells for 24 h in the presence of c-Met/PD-1 CAR-T supernatant, apoptosis was significantly reduced compared to Active T cells without the supernatant (Fig. 5). Specifically, the apoptosis rate of T cells co-cultured with ECA109 cells decreased from 44.70 ± 1.73% to 9.78 ± 0.97%, with the difference being statistically significant ($P < 0.05$).

3.7 The ability of T cells to expand in the presence of antigen

As shown in Table 4, after 24 h of co-culture, there was no significant difference in the proliferation of the different T cells (Fig. 6A). However, after 48 h of co-culture, the number of effector cells in the c-Met/PD-1 CAR-T group was significantly increased than that in the CD19 CAR-T and Active T cell groups. After 72 h of co-culture, the

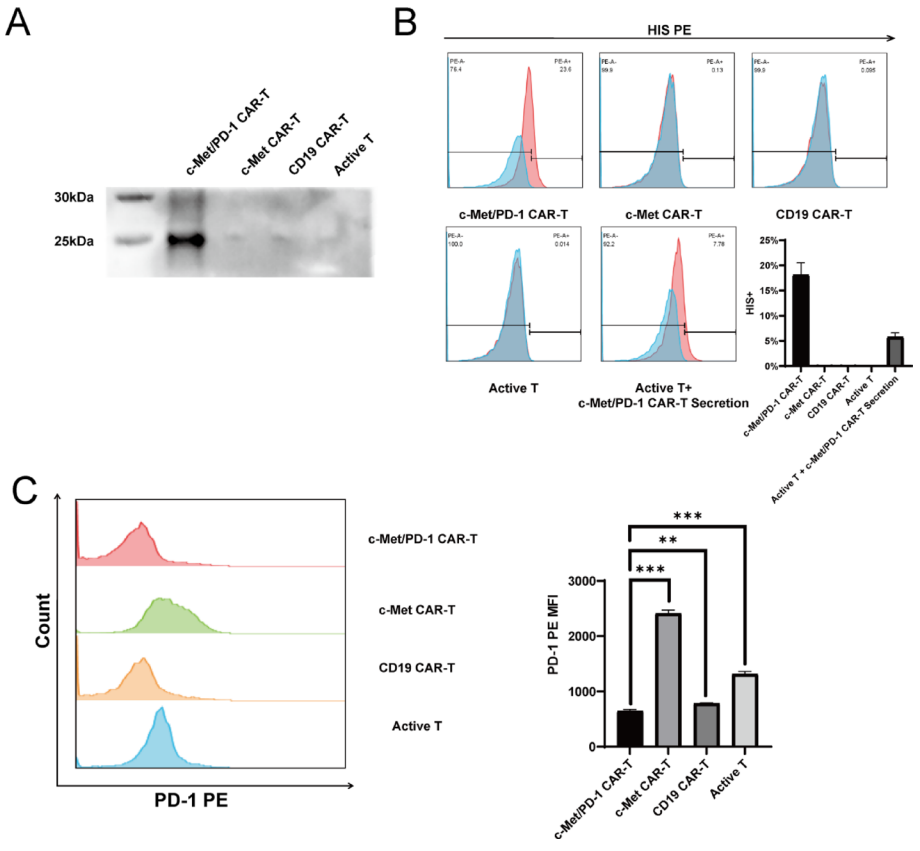

Fig. 4 PD-1 Antibody Secretion and Binding. **A** Western blot detection of HIS tag in CAR-T cell supernatants; **B** Flow cytometry detection of HIS tag on the surface of CAR-T cells; C: Flow cytometry detection of PD-1 mean fluorescence intensity on the surface of CAR-T cells, analyzed by one-way ANOVA, (**$P < 0.01$, ***$P < 0.001$, $n = 3$)

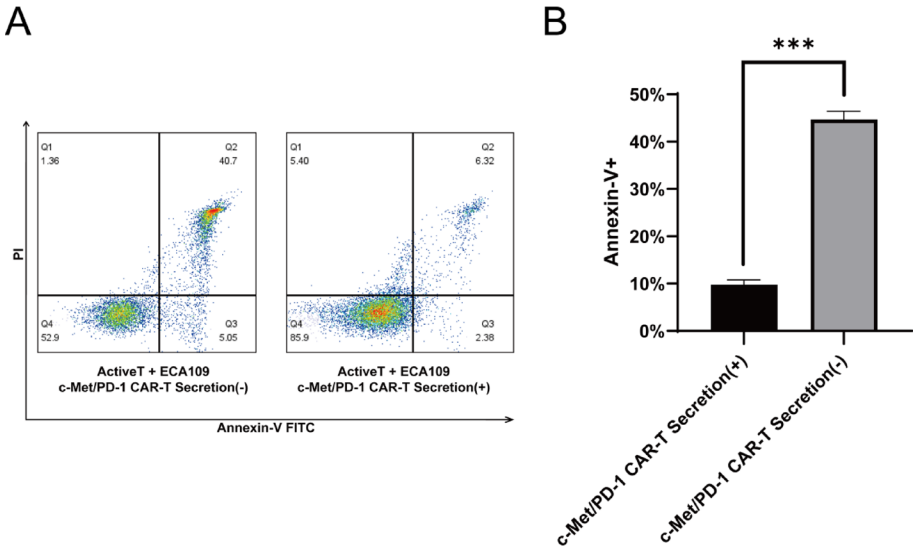

Fig. 5 Flow Cytometry Analysis of Apoptosis in Active T Cells Co-cultured with ECA109 Cells in c-Met/PD-1 CAR-T Supernatant analyzed by one-way ANOVA, ***$p < 0.001$, $n = 3$

Table 4 Proliferation of various T cells stimulated by cancer cells

Group	Number of Effector Cells			
	0 h	24 h	48 h	72 h
c-Met/PD-1 CAR-T + ECA109	0.5×10^5	$(1.05 \pm 0.21) \times 10^5$	$(2.21 \pm 0.12) \times 10^5$	$(3.14 \pm 0.16) \times 10^5$
c-Met CAR-T + ECA109	0.5×10^5	$(1.13 \pm 0.1) \times 10^5$	$(1.93 \pm 0.12) \times 10^5$	$(2.43 \pm 0.17) \times 10^5$
CD19 CAR-T + ECA109	0.5×10^5	$(0.71 \pm 0.14) \times 10^5$	$(1.17 \pm 0.13) \times 10^5$	$(1.38 \pm 0.08) \times 10^5$
Active T + ECA109	0.5×10^5	$(0.86 \pm 0.09) \times 10^5$	$(1.1 \pm 0.22) \times 10^5$	$(1.38 \pm 0.2) \times 10^5$

proliferation capacity of c-Met/PD-1 CAR-T cells was significantly increased than that of c-Met CAR-T, CD19 CAR-T, and Active T cells, with the difference being statistically significant ($P<0.05$).

3.8 In vitro toxicity of c-Met/PD-1 CAR-T cells in ESCA

After co-culturing CAR-T cells with ECA109 cells for 6 h, the killing ability of CAR-T cells against cancer cells was assessed, and the results are shown in Table 5. We found that at all effector-to-target ratios, the killing efficiency of c-Met/PD-1 CAR-T cells was significantly increased than that of CD19 CAR-T and Active T cells (Fig. 6B). At an effector-to-target ratio of 20:1, the PD-1 antibody played a protective role, with the killing rate of c-Met/PD-1 CAR-T cells reaching 56.93 ± 3.67%, which was significantly increased than that of c-Met CAR-T cells without secretion function, with the difference being statistically significant ($P < 0.05$).

To further confirm the effectiveness of c-Met/PD-1 CAR-T cells, we employed ELISA to measure the cytokine secretion capacity of c-Met/PD-1 CAR-T cells stimulated by ECA109 cells. After co-culturing CAR-T cells with ECA109 cells for one day, supernatants were collected and the levels of IL-2, IFN-γ, and TNF-α were detected (Fig. 6C). The concentrations of IL-2 and IFN-γ secreted by c-Met/PD-1 CAR-T cells co-cultured with ECA109 were 494.14 ± 11.36 pg/ml and 1298.16 ± 95.53 pg/ml, respectively, while the concentration of TNF-α was 112.33 ± 17.93 pg/ml. We found that the levels of IL-2 and IFN-γ secreted by c-Met/PD-1 CAR-T cells were significantly increased than those

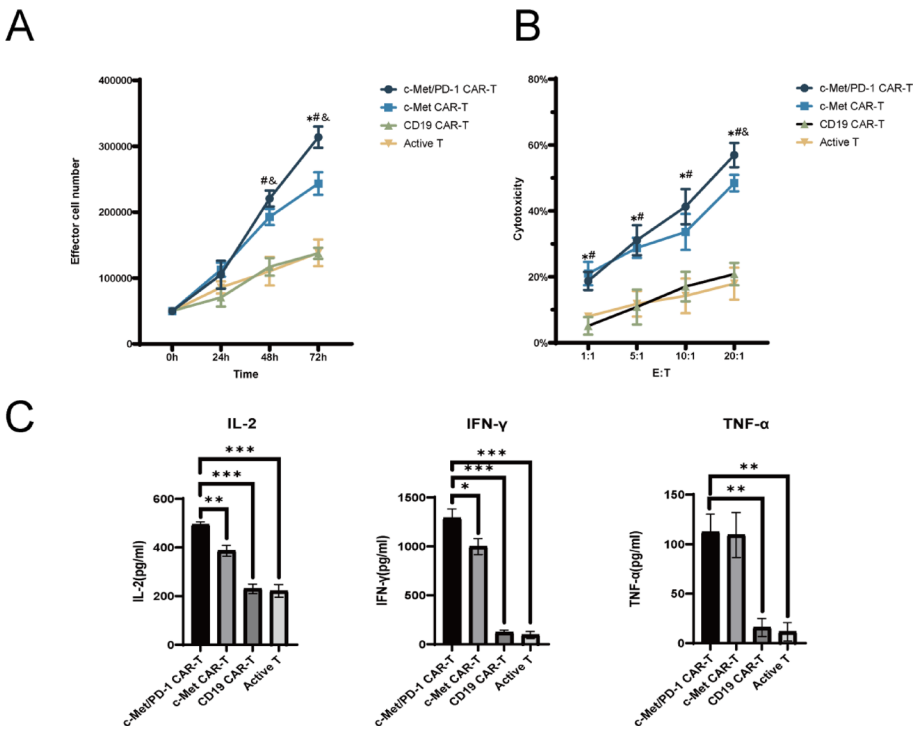

Fig. 6 In Vitro Functional Assays of c-Met/PD-1 CAR-T Cells. **A** CCK-8 assay showing the proliferation curve of c-Met/PD-1 CAR-T cells co-cultured with ECA109 cells analyzed by two-way ANOVA, $*p<0.05$ vs. c-Met CAR-T; $\#p<0.05$ vs. CD19 CAR-T; $\&p<0.05$ vs. Active T, $n=3$; **B** LDH assay showing the killing efficiency curve of c-Met/PD-1 CAR-T cells co-cultured with ECA109 cells at different effector-to-target ratios. analyzed by two-way ANOVA, $\&p<0.05$ vs. c-Met CAR-T; $\#p<0.05$ vs. CD19 CAR-T; $*p<0.05$ vs. Active T, $n=3$; **C** ELISA assay showing the cytokine release of c-Met/PD-1 CAR-T cells co-cultured with ECA109 cells analyzed by one-way ANOVA, $*p<0.05$, $**p<0.01$, $***p<0.001$, $n=3$

Table 5 CAR-T killing efficiency at various effector-to-target ratios

Group	E: T			
	1:1	5:1	10:1	20:1
c-Met/PD-1 CAR-T + ECA109	(18.74 ± 2.74)%	(31.1 ± 4.53)%	(41.29 ± 5.32)%	(56.93 ± 3.67)%
c-Met CAR-T + ECA109	(20.97 ± 3.54)%	(28.77 ± 3.03)%	(33.62 ± 5.46)%	(48.43 ± 2.48)%
CD19 CAR-T + ECA109	(5.11 ± 2.67)%	(10.84 ± 5.29)%	(17.05 ± 4.49)%	(20.83 ± 3.4)%
Active T + ECA109	(7.98 ± 0.98)%	(11.82 ± 3.86)%	(14.22 ± 5.25)%	(17.92 ± 4.86)%

secreted by c-Met CAR-T, CD19 CAR-T, and Active T cells. The secretion of TNF-α by c-Met/PD-1 CAR-T cells was not significantly different from that of c-Met CAR-T cells but was significantly increased than that of CD19 CAR-T and Active T cells, with the difference being statistically significant ($P<0.05$).

3.9 Effect of c-Met/PD-1 CAR-T cells on ESCA xenografts in nude mice

On the 14th day after subcutaneous injection of ECA109-luc cells into the axillae of nude mice, 20 tumor-bearing mice were selected and evenly divided into four groups, utilizing a tumor volume of 100 mm^3 as the standard. Each group received two injections of c-Met/PD-1 CAR-T, c-Met CAR-T, Active T cells, or PBS at 7-day intervals (Fig. 7A). During the entire study, no mice were found to be in poor health or experienced mortality, and there was no statistical difference in weight change (Fig. 7B). Bioluminescence imaging demonstrated that the fluorescence intensity in the c-Met/PD-1 CAR-T

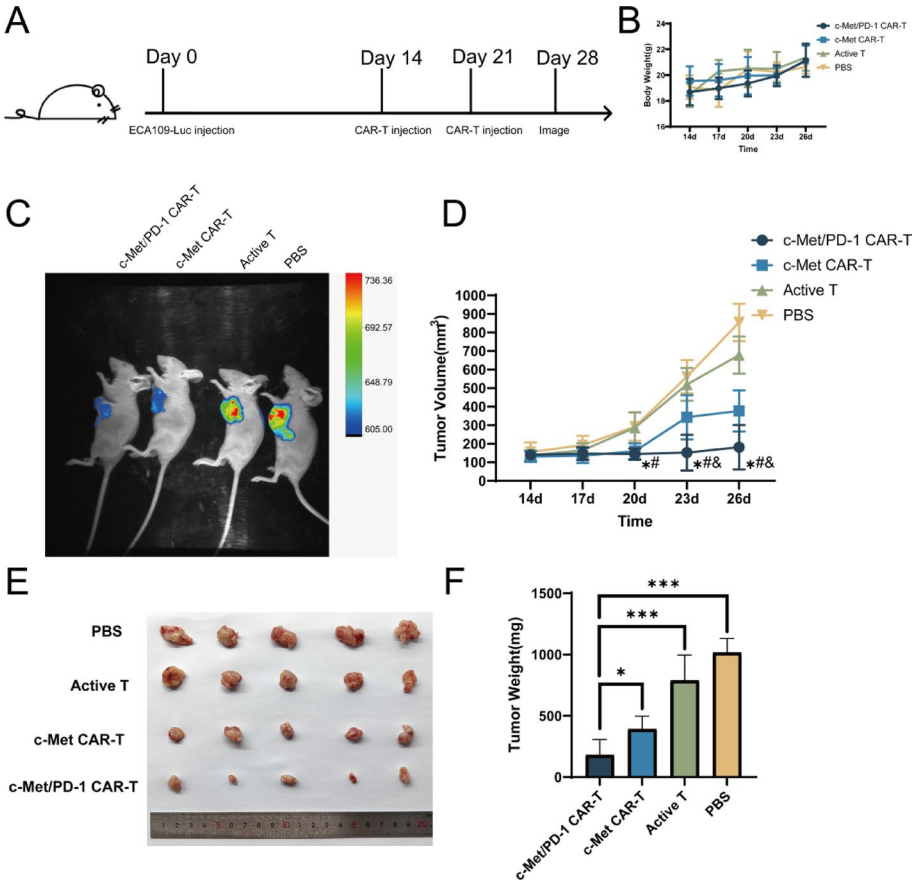

Fig. 7 In Vivo Treatment of Tumor-Bearing Nude Mice with c-Met/PD-1 CAR-T Cells. **A** Schematic diagram of the in vivo experiment process; **B** Line graph showing changes in body weight of nude mice; **C** Bioluminescence imaging of ECA109-Luc subcutaneous xenograft model; **D** Statistical analysis of tumor volume at different time points (analyzed by two-way ANOVA,&$p < 0.05$ vs. c-Met CAR-T; #$p < 0.05$ vs. CD19 CAR-T; *$p < 0.05$ vs. PBS, $n = 5$); **E** Images of excised xenografts from each group after treatment; F: Tumor mass of each group after treatment (analyzed by one-way ANOVA, *$p < 0.05$, **$p < 0.01$, ***$p < 0.001$, $n = 5$)

treatment group was significantly decreased than that in the Active T cell and PBS groups (Fig. 7C). Dynamic monitoring of tumor volume demonstrated that the tumor volume in the c-Met/PD-1 CAR-T treatment group was smaller than that in the Active T cell treatment group after day 20, and smaller than that in the c-Met CAR-T treatment group after day 23, with the differences being statistically significant ($P < 0.05$) (Fig. 7D). After euthanizing the mice and extracting the tumors (Fig. 7E, F), the tumor weight in the c-Met/PD-1 CAR-T treatment group was 180.86 ± 125.93 g, which was significantly decreased than that in the c-Met CAR-T treatment group (391.94 ± 104.54 mg), the Active T cell treatment group (788.2 ± 206.84 mg), and the PBS injection group (1016.82 ± 114.01 mg), with the differences being statistically significant ($P < 0.05$).

On day 28, after euthanizing the nude mice, heart, liver, spleen, lung, and kidney tissues were collected and subjected to HE staining (Fig. 8). In the c-Met/PD-1 CAR-T cell treatment group, the myocardial tissue of the heart demonstrated a regular striated structure, with tightly arranged myocardial cells containing centrally located oval nuclei. The intercellular matrix was sparse, and no significant infiltration of inflammatory cells or fibrosis was observed. In the liver, the hepatic lobule structure was regular, with hepatocytes arranged radially around the central vein. The hepatocytes exhibited a typical

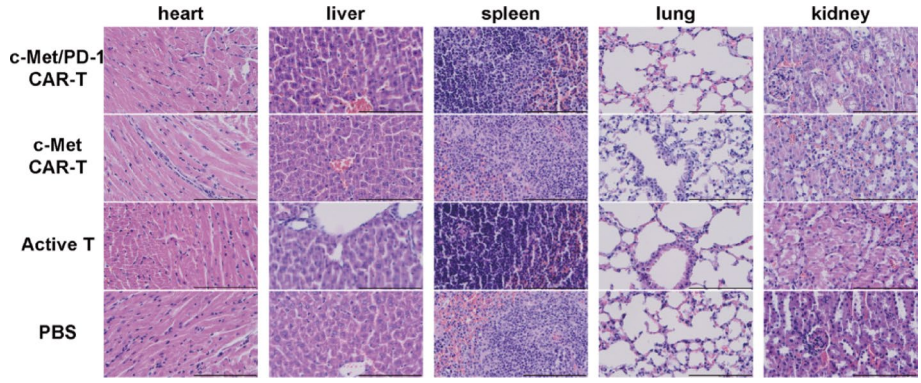

Fig. 8 HE Staining of Major Organs in Nude Mice from Each Treatment Group (×400)

polygonal shape with centrally located nuclei and clear cytoplasm, with no significant necrosis or inflammatory changes. In the spleen, the boundaries between the white pulp and red pulp were clear, with densely packed lymphocytes in the white pulp region and blood cells filling the red pulp. No obvious pathological changes were observed. The lung alveolar structure was intact, with thin alveolar walls rich in capillaries and neatly arranged alveolar epithelial cells. No significant fibrosis, alveolar rupture, or congestion was detected. The kidney glomeruli demonstrated intact structures, with no signs of proliferation or sclerosis. The renal tubule structures were normal, with neatly arranged cells and no apparent signs of cell degeneration or necrosis.

4 Discussion

Surgery remains the main treatment for early ESCA, improving 5-year survival rates to 60%-85% in patients with high-grade dysplasia and very early tumors [22]. However, early diagnosis of esophageal cancer is challenging due to the rich lymphatic drainage in the submucosa, leading to early lymph node metastasis. For advanced esophageal cancer, surgery combined with chemoradiotherapy (CRT) offers a 5-year survival rate of approximately 50% but is associated with high recurrence rates and reduced quality of life. CAR-T therapy, with its specificity, memory, and personalized advantages, is more suitable for treating advanced ESCA.

Chimeric antigen receptors (CARs) are fusion proteins consisting of an extracellular antigen recognition domain and an intracellular T cell activation domain. The extracellular domain is usually an scFv targeting tumor cell surface molecules, while the intracellular domain typically includes CD3ζ and co-stimulatory domains like CD28, CD137, or CD134, which significantly enhance the survival of CAR-T cells [23, 24]. This synthetic tumor-targeting receptor allows transgenic T cells to perform anti-tumor functions in a non-MHC-restricted manner [25]. Despite the success of CAR-T cell immunotherapy in hematological malignancies, the efficacy of CAR-T cells in solid tumors remains unsatisfactory due to antigen escape effects .

In recent studies, Keishi Adachi et al. constructed CARs secreting IL-7 and CCL19, demonstrating superior killing effects on mast cell tumors compared to CD20 monoclonal antibody CAR-T cells [26]. Similarly, Sarwish Rafiqi et al. developed PD-1 scFv-secreting CARs with stronger in vitro and in vivo anti-tumor activity than conventional CAR-T cells [27]. Thus, constructing secreting CARs combined with immune checkpoint inhibitors is an effective strategy to enhance CAR-T therapy for solid tumors.

TCGA database, immunohistochemistry, and flow cytometry results demonstrated high expression of c-Met and PD-L1 in esophageal cancer. Several c-Met-targeted antibodies, such as Tepotinib, Capmatinib, Rybrevant, and Rilotumumab, have been reported. Our early work successfully constructed anti-human c-Met scFvs, which targeted c-Met protein on tumor cells and significantly inhibited c-Met-positive non-small cell lung cancer cells in vitro and in vivo [28]. However, under c-Met-targeted drug action, tumor cells activate alternative signaling pathways (e.g., EGFR, HER2/neu, PI3K/AKT/mTOR), leading to drug resistance [29]. Additionally, targeted drugs only block corresponding pathways, inhibiting cancer cell proliferation, spread, and recurrence [30], but cannot induce cancer cell apoptosis.

In our early work, we constructed c-Met-targeted CAR-T cells, which exhibited killing effects on c-Met-positive non-small cell lung cancer cells and colon cancer cells in vitro and in vivo [15, 31]. However, efficacy was limited, with improvements needed in T cell survival and treatment durability.

PDCD1 and CD274 encode PD-1 and PD-L1, respectively, and their upregulated expression in tumors is multifaceted. Activation of tumor-related signaling pathways, such as PI3K/AKT, MAPK, and JAK/STAT, upregulates PD-L1 expression. Additionally, inflammatory cytokines (e.g., IL-6, TNF-α) and acidic conditions in the tumor microenvironment further increase PD-1/PD-L1 expression [32]. Chronic inflammation, such as reflux esophagitis or Barrett's esophagus, is associated with esophageal cancer, with cytokines inducing PD-L1 expression upregulation [33]. Given the challenges of immune escape in solid tumors, combination therapies, such as PD-1 inhibitors and CAR-T cells, are emerging as promising strategies. In particular, the combination of PD-1-TREM2 scFv with CAR-T cells has been shown to not only enhance the therapeutic efficacy against colorectal cancer (CRC) but also overcome immune escape by reducing immunosuppressive cells (e.g., MDSCs and TAMs) within the tumor microenvironment [34]. This study highlights the potential of dual-targeting PD-1 and c-Met, offering a novel approach to enhance CAR-T therapy for esophageal cancer. The PD-1 antibody secreted by c-Met-targeted CAR-T cells may help prevent T cell exhaustion induced by the PD-1/PD-L1 interaction, improving T cell persistence and activity within the tumor, thus overcoming antigen loss and enhancing therapeutic efficacy. Therefore, this study selected c-Met and PD-1 as target antigens.

We connected the c-Met CAR sequence to the PD-1 antibody secretion sequence via FP2A and transfected the CAR sequence into T cells utilizing lentiviral vectors. Flow cytometry confirmed successful construction and expression of PD-1 antibody-secreting c-Met CAR-T cells. Under a single promoter, CAR and PD-1 antibody were translated, cleaved at FP2A, and secreted extracellularly, binding to PD-1 on T cells. However, it is important to note that the inclusion of the PD-1 antibody sequence resulted in an increase in the overall length of the CAR sequence. This structural modification likely affected the efficiency of lentiviral transduction, leading to lower transduction rates for the c-Met/PD-1 CAR-T cells compared to second-generation CAR-T cells without the additional PD-1 antibody sequence. As a result, the observed superior effects of the c-Met/PD-1 CAR-T cells may actually be even stronger than reported, but the lower CAR expression complicates direct comparisons with other CAR-T constructs. The impact of this transduction efficiency difference should be carefully considered when interpreting the data. Western blot and flow cytometry results confirmed that PD-1

antibodies were secreted extracellularly, reducing T cell apoptosis when co-cultured with cancer cells. Interestingly, this protective effect is composed of two parts: autocrine and paracrine mechanisms. First, the PD-1 antibody secreted by the CAR-T cells directly binds to the PD-1 sites on the CAR-T cell surface, thereby enhancing their activity. Second, through a paracrine effect, the secreted PD-1 antibody binds to the PD-1 sites on normal T cells, blocking the PD-1/PD-L1 pathway, and counteracting the tumor cells' immune cell exhaustion effects.

Subsequent LDH assays demonstrated that c-Met/PD-1 CAR-T cells exhibited significantly increased in vitro killing activity against c-Met/PD-L1-positive ECA109 cells compared to traditional c-Met CAR-T cells, CD19 CAR-T cells, and Active T cells. CCK-8 assays confirmed the enhanced proliferation ability of c-Met/PD-1 CAR-T cells under c-Met antigen stimulation compared to other groups. ELISA results demonstrated that c-Met/PD-1 CAR-T cells secreted significantly increased levels of IFN-γ and IL-2 than other groups. These results collectively suggested that PD-1 antibodies protected T cells by maintaining T cell activity, inhibiting apoptosis, increasing cell numbers, and enhancing in vitro anti-tumor effects.

In animal models, c-Met/PD-1 CAR-T-treated mice demonstrated no abnormalities, stable body weight, and significantly decreased tumor growth compared to other groups. Tumor volume was significantly smaller in the c-Met/PD-1 CAR-T group, indicating enhanced killing effects compared to traditional c-Met CAR-T cells and CD19 CAR-T cells. HE staining demonstrated no significant damage to normal organs, indicating the safety of c-Met/PD-1 CAR-T cells. These conclusions were supported by Rafiq et al., who observed that PD-1 antibody secreted by CAR-T cells localized mainly in the tumor, avoiding systemic toxicity [27].

However, it is important to note that the use of nude mouse models in this study has certain limitations. Nude mice lack a functional T-cell compartment, which means the model cannot recapitulate the complex interactions between CAR-T cells and the host immune system (NK cells, macrophages, dendritic cells) that occur in the TME. The benefit of blocking the PD-1/PD-L1 axis is likely underestimated in a model that lacks endogenous PD-1 expressing T-cells. Therefore, we plan to use more advanced immunocompetent mouse models in future studies to more accurately assess the role of the PD-1/PD-L1 pathway in CAR-T cell therapy and better reflect the immune interactions present in human cancers.

Currently, no CAR-T therapy for esophageal cancer has been reported. Only five studies have introduced second-generation CAR-T therapies targeting EGFR [35], HER2 [36], EphA2 [37], MUC1 [38], CD276 [39] for esophageal cancer in preclinical research, with significant inhibitory effects on esophageal cancer cells. However, these targets are also expressed in adjacent tissues, posing off-target risks. c-Met CAR construction has been reported fornasopharyngeal carcinoma, demonstrating anti-tumor effects in vitro and in vivo [40]. However, no studies have reported utilizing c-Met as a CAR-T target for esophageal cancer. To address immune escape, we preliminarily constructed c-Met/PD-1 CAR-T cells and evaluated their efficacy and safety in vitro and in vivo. Despite promising results, limitations remain. Establishing an orthotopic esophageal cancer model would more effective simulate real conditions. Additionally, the use of nude mice, lacking normal immune function, suggests considering other mouse models. Given that

c-Met and PD-L1 are tumor-associated antigens with low expression in normal esophageal cells, further safety evaluations are necessary.

In conclusion, we successfully constructed c-Met/PD-1 CAR-T cells, demonstrating significant in vitro and in vivo killing effects on c-Met/PD-L1-positive esophageal cancer cells. These findings indicate potential applications for c-Met/PD-1 CAR-T cell immunotherapy in ESCA. However, further validation in more animal models and clinical trials is required to confirm efficacy, address antigen escape, homing, and tumor microenvironment maintenance challenges. With advances in gene editing and combination therapies, c-Met/PD-1 CAR-T cells could become a new approach for ESCA treatment.

Abbreviations

PD-1	Programmed death-1
c-Met	Cellular-mesenchymal to epithelial transition factor
CAR-T	Chimeric antigen receptor T cell
ECA109	Esophageal cancer cell line 109
TCGA	The cancer genome atlas
GTEx	Genotype-tissue expression
HE	Hematoxylin and Eosin
CCK-8	Cell counting kit-8
ELISA	Enzyme-linked immunosorbent assay
LDH	Lactate dehydrogenase
PBS	Phosphate-buffered saline
SPF	Specific pathogen-free
MOI	Multiplicity of infection
PBMC	Peripheral blood mononuclear cells
FP2A	Foot-and-mouth disease virus 2 A
GFP	Green fluorescent protein
IFN-γ	Interferon-gamma
IL-2	Interleukin-2
IL-7	Interleukin-7
IL-15	Interleukin-15
TNF-α	Tumor necrosis factor-alpha
ARRIVE	Animal research: reporting of in vivo experiments
EGFR	Epidermal growth factor receptor
MUC1	Mucin 1
CD276	Cluster of differentiation 276
ERBB2	Erb-B2 receptor tyrosine kinase 2
HER2	Human epidermal growth factor receptor 2
EphA2	Ephrin type-A receptor 2

Acknowledgements
Not applicable.

Author contributions
Shang Peng (S.P.): Study design, gene expression analysis, and drafting the manuscript.Yanqiu Li (Y.L.): Conducted in vitro and cellular experiments, and contributed to manuscript writing.Yanjun Zhang (Y.Z.): Statistical analysis and figure preparation, involved in study design and manuscript revision.Jingting Min (J.M.): Constructed and prepared c-Met/PD-1 CAR-T cells, participated in in vivo experiments and data collection.Ran An (R.A.): Performed immunohistochemistry and protein experiments, supported data analysis.Nana Du (N.D.): Collected tissue samples, conducted immunohistochemistry, and provided statistical support.Haipeng Li (H.L.): Managed in vivo mouse experiments, established tumor models, and administered CAR-T cells.Xiangcheng Zhen (X.Z.): Conducted cytokine release and flow cytometry assays, contributed to the discussion section.Fei Chu (F.C.): Bioinformatics analysis and data visualization, contributed to manuscript writing.Zhenghong Li (Z.L.) (corresponding author): Supervised the project, study design, data interpretation, and manuscript coordination.Each author played a critical role in various aspects of the research, contributing to the overall success of the project.

Funding
Key Research Project of Higher Education Institutions in Anhui Province (2023AH051991); Major Project of Natural Science Research in Anhui Provincial Universities (2022AH040224); Graduate Student Innovation Project of Bengbu Medical College (Byycx22015); National Undergraduate Innovation and Entrepreneurship Projects (202310367011);Bengbu Medical College Natural Science Project(2021byzd015).

Data availability
The datasets used and/or analysed during the current study available from the corresponding author on reasonable request.

Declarations

Ethics approval and consent to participate
The human research component of this study was approved by the Ethics Committee of Bengbu Medical University (Approval No. Lunke [2022] No. 115). All tissue samples were anonymized before use in this study, and no identifiable personal information was accessed during or after the research. The Ethics Committee waived the need for additional informed consent for the use of these archived samples in retrospective research. The animal experiments were approved by the Animal Ethics Committee of Bengbu Medical University (Approval No. Lundongke [2022] No. 191) and were conducted in accordance with relevant ethical guidelines and regulations for the management of laboratory animals. All methods involving human participants were carried out in accordance with relevant guidelines and regulations. The Ethics Committee waived the need for additional informed consent for the use of these archived samples in retrospective research.

Consent for publication
Not applicable. This study does not involve any individual data that requires consent for publication.

Competing interests
The authors declare no competing interests.

Received: 30 April 2025 / Accepted: 25 September 2025
Published online: 21 October 2025

References

1. Mönig S, Chevallay M, Niclauss N, et al. Early esophageal cancer: the significance of surgery, endoscopy,and chemoradiation. Ann N Y Acad Sci. 2018;1434:115–23.
2. Omloo JM, Lagarde SM, Hulscher JB, et al. Extended transthoracic resection compared with limited transhiatal resection for adenocarcinoma of the mid/distal esophagus: five-year survival of a randomized clinical trial. Ann Surg. 2007;246:992–1000.
3. Oppedijk V, van der Gaast A, van Lanschot JJ, et al. Patterns of recurrence after surgery alone versus preoperative chemoradiotherapy and surgery in the CROSS trials. J Clin Oncol. 2014;32:385–91.
4. Chen G, Wang Z, Liu XY, Liu FY. Recurrence pattern of squamous cell carcinoma in the middle thoracic esophagus after modified Ivor-Lewis esophagectomy. World J Surg. 2007;31:1107–14.
5. Haslauer T, Greil R, Zaborsky N, Geisberger R. CAR T-Cell therapy in hematological malignancies. Int J Mol Sci. 2021;22(16):8996.
6. Melenhorst JJ, et al. Decade-long leukaemia remissions with persistence of CD4 + CAR T cells. Nat [J]vol. 2022;602(7897):503–9. https://doi.org/10.1038/s41586-021-04390-6.
7. Depil S, Duchateau P, Grupp SA, Mufti G, Poirot L. Off-the-shelf' allogeneic CAR T cells: development and challenges. Nat Rev Drug Discov. 2020;19(3):185–99.
8. Aparicio-Pérez C, Carmona M, Benabdellah K, Herrera C. Failure of ALL recognition by CAR T cells: a review of CD 19-negative relapses after anti-CD 19 CAR-T treatment in B-ALL. Front Immunol. 2023;14:1165870.
9. Safarzadeh Kozani P, Safarzadeh Kozani P, Ahmadi Najafaunsatisfactoryi M, et al. Recent advances in solid tumor CAR-T cell therapy: driving tumor cells from hero to zero? Front Immunol. 2022;13:795164.
10. Wagner J, Wickman E, DeRenzo C, et al. CAR T cell therapy for solid tumors: bright future or dark reality? Mol Ther. 2020;28(11):2320–39.
11. Febres-Aldana CA, Vojnic M, Odintsov I, et al. Pan-Cancer analysis of oncogenic MET fusions reveals distinct pathogenomic subsets with differential sensitivity to MET-Targeted therapy. Cancer Discov. 2025;15(6):1141–58.
12. Guo R, Luo J, Chang J, Rekhtman N, et al. MET-dependent solid tumours - molecular diagnosis and targeted therapy. Nat Rev Clin Oncol. 2020;17(9):569–87.
13. Alunsatisfactoryari N, Xie Y, Li W. Deciphering treatment resistance in metastatic colorectal cancer: roles of drug transports, EGFR mutations, and HGF/c-MET signaling. Front Pharmacol. 2024;14:1340401.
14. Camargo MC, Song M, Ito H, et al. Associations of Circulating mediators of inflammation, cell regulation and immune response with esophageal squamous cell carcinoma. J Cancer Res Clin Oncol. 2021;147(10):2885–92.
15. Min J, Long C, Zhang L, et al. c-Met specific CAR-T cells as a targeted therapy for non-small cell lung cancer cell A549. Bioengineered. 2022;13(4):9216–32.
16. Zhou Y, Wei S, Xu M, et al. CAR-T cell therapy for hepatocellular carcinoma: current trends and challenges. Front Immunol. 2024;15:1489649.
17. Chen C, Gu YM, Zhang F, et al. Construction of PD1/CD28 chimeric-switch receptor enhances anti-tumor ability of c-Met CAR-T in gastric cancer. Oncoimmunology. 2021;10(1):1901434.
18. Atrash S, Bano K, Harrison B et al. CAR-T treatment for hematological malignancies. J Investig Med. 2020;68(5): 956–64.
19. Pan EY, Merl MY, Lin K. The impact of corticosteroid use during anti-PD1 treatment. Oncol Pharm Pract. 2020;26(4):814–22.
20. Rossjohn J, Gras S, Miles JJ, et al. The Anti-PD-1/PD-L1 immunotherapy for gastric esophageal cancer: A systematic review and Meta-Analysis and literature review. Cancer Control. 2021;28:1073274821997430.
21. Dhillon S, Ivonescimab: First Approval. Drugs. 2024;84(9):1135–42.
22. Plum PS, Hölscher AH, Pacheco Godoy K, et al. Prognosis of patients with superficial T1 esophageal cancer who underwent endoscopic resection before esophagectomy-A propensity score-matched comparison. Surg Endosc. 2018;32:3972–80.
23. Zhang X, Zhu L, Zhang H, Chen S, Xiao Y. CAR-T cell therapy in hematological malignancies: current opportunities and challenges. Front Immunol. 2022;13:927153.
24. Ma S, Li X, Wang X, et al. Current progress in CAR-T cell therapy for solid tumors. Int J Biol Sci. 2019;15(12):2548–60.
25. Dai X, Mei Y, Cai D, et al. Standardizing CAR-T therapy: getting it scaled up. BiotechnolAdv. 2019;37(1):239–45.

26. Adachi K, Kano Y, Nagai T, et al. IL-7 and CCL19 expression in CAR-T cells improves immune cell infiltration and CAR-T cell survival in the tumor. Nat Biotechnol. 2018;36(4):346–51.
27. Rafiq S, Yeku OO, Jackson HJ, et al. Targeted delivery of a PD-1-blocking ScFv by CAR-T cells enhances anti-tumor efficacy in vivo. Nat Biotechnol. 2018;36(9):847–56.
28. An R, Liu M, Zhang L et al. Intraperitoneal injection of humanized anti-c-Met single-chain antibody inhibits the growth of A549 lung adenocarcinoma xenografts in mice. Chin J Cell Mol Immunol. 40(06):549–55.
29. Wu YL, Cheng Y, Zhou J et al. Tepotinib plus gefitinib in patients with EGFR-mutant non-small-cell lung cancer with MET overexpression or MET amplification and acquired resistance to previous EGFR inhibitor (INSIGHT study): an open-label, phase 1b/2, multicentre, randomised trial. Lancet Respir Med. 2020;8(7):e59.
30. Letai A, Bhola P, Welm AL. Functional precision oncology: testing tumors with drugs to identify vulnerabilities and novel combinations. Cancer Cell. 2022;40(1):26–35.
31. Peng S, Min JT, Long CR et al. Bioinformatics prediction and validation of cellular mesenchymal-epithelial transition factor (c-Met) as a target for chimeric antigen receptor T (CAR-T) cell therapy in colorectal cancer. Chin J Cell Mol Immunol [J/OL], 1–15 [2024-08-21].
32. Nallasamy P, Chava S, Verma SS, et al. PD-L1, inflammation, non-coding RNAs, and neuroblastoma: Immuno-oncology perspective. Semin Cancer Biol. 2018;52(Pt 2):53–65.
33. Ozawa Y, Nakamura Y, Fujishima F, et al. c-Met in esophageal squamous cell carcinoma: an independent prognostic factor and potential therapeutic target. BMC Cancer. 2015;15:451.
34. Chen J, Zhu T, Jiang G, Zeng Q, Li Z, Huang X. Target delivery of a PD-1-TREM2 ScFv by CAR-T cells enhances anti-tumor efficacy in colorectal cancer. Mol Cancer. 2023;22(1):131.
35. Cheng C, Cui H, Liu H, et al. Role of epidermal growth factor Receptor-Specific CAR-T cells in the suppression of esophageal squamous cell carcinoma. Cancers (Basel). 2022;14(24):6021.
36. Xuan Y, Sheng Y, Zhang D, et al. Targeting CD276 by CAR-T cells induces regression of esophagus squamous cell carcinoma in xenograft mouse models. Transl Oncol. 2021;14(8):101138.
37. Shi H, Yu F, Mao Y, et al. EphA2 chimeric antigen receptor-modified T cells for the immunotherapy of esophageal squamous cell carcinoma. J Thorac Dis. 2018;10(5):2779–88.
38. Yu F, Wang X, Shi H, et al. Development of chimeric antigen receptor-modified T cells for the treatment of esophageal cancer. Tumori. 2021;107(4):341–52.
39. Rajabzadeh A, Hamidieh AA, Rahbarizadeh F. Spinoculation and retronectin highly enhance the gene transduction efficiency of Mucin-1-specific chimeric antigen receptor (CAR) in human primary T cells. BMC Mol Cell Biol. 2021;22(1):57.
40. Huo Q, Lv J, Zhang J, et al. c-Met is a chimeric antigen receptor T-cell target for treating recurrent nasopharyngeal carcinoma. Cytotherapy. 2023;25(10):1037–47.

Publisher's note